

A Momentum Space View of the Surface Chemical Bond - Supplementary Information

Stephen Berkebile,^a Thomas Ules,^a Peter Puschnig,^b Lorenz Romaner,^b Georg Koller,^a Alexander J. Fleming,^a Konstantin Emtsev,^c Thomas Seyller,^c Claudia Ambrosch-Draxl,^b Falko P. Netzer,^a and Michael G. Ramsey^{*a}

Contents

A Valence Band — Cu[001]	1
B Beyond the Monolayer	2
C Modifying the Periodicity	3
D Theoretical Support	3
D.1 Orbital Character Calculation	3
D.2 Localized π orbitals	4
D.3 Torsional Angle	4

A Valence Band — Cu[001]

Figure S1 shows the photoemission intensity map $E(k_y)$ in the Cu[001] direction, the azimuthal plane perpendicular to that of Fig. 3. For the clean Cu(110) surface in (a), the s,p and d bands can be observed as described above with the additional presence of the Shockley surface state located around E_F and the $\bar{\Gamma}_{\text{Cu}}$ Brillouin zone (BZ) boundary in the gap of the bulk band structure projection on the surface. This surface state appears as a parabola running from $k_y \approx 0.8$ to 1.0 \AA^{-1} and between E_F and $E_B = -0.4 \text{ eV}$.

When the monolayer of 6P has been deposited (Fig. S1b), the molecular axis is perpendicular to this azimuth. Consequently, strong distinct emissions from the HOMO and the rest of its associated π band are not observed, similar to the photoemission behavior of the multilayer in the same geometry (see Ref. [1]). Emissions from the Cu d band region are altered and have become indistinct. In the calculations of Section D.2, the six localized π orbitals are essentially energetically degenerate and display a double peaked, flat band structure with a splitting of $\approx 1.1 \text{ eV}$. Following symmetry arguments, at least the HOMO-8 of the localized π orbitals should be apparent in photoemission in this geometry due to the lack of a nodal plane in the y -direction. Unlike multilayer films, no

^{0a} Karl-Franzens University, Universitätsplatz 5, 8010 Graz, Austria. E-mail: ramsey@uni-graz.at

^{0b} University of Leoben, Leoben, Austria.

^{0c} University of Erlangen-Nürnberg, Erlangen, Germany.

strong dispersion of the localized orbitals can be observed (compare to Ref. [1]). What is observed here is that, in both the d band region and near the $\bar{\Gamma}$ point in the s and p band regions, the emission features appear with a periodicity of the scattering vector associated with the 7.2 Å overlayer periodicity observed in LEED of $\mathbf{G} = 2\pi/7.2 \text{ \AA} = 0.87 \text{ \AA}^{-1}$ (a vector \mathbf{G} has been added to Fig. S1b for clarity). Whether these features arise purely from a band folding of the Cu features on the overlayer structure, or indeed arise from molecular π orbitals is an issue which cannot be resolved here. As only the HOMO-8 orbital (of the localized orbitals) should be observed in photoemission in this symmetry plane, it seems that the former possibility is likely, therefore demonstrating that changes in the photoemission features upon adsorption do not necessarily arise from molecular features.

Upon molecular adsorption, the surface state at the \bar{Y} BZ boundary is no longer observed near E_F , leaving the gap in the bulk band structure in which it was located apparent as an area of lower intensity up to 0.5 eV below E_F . Similar to the other azimuthal geometry, strong emissions also appear near E_F , however here they have a large k -spread from $k_y = 1.0$ to 2.5 \AA^{-1} in this geometry. As discussed in the main article, these emissions also originate from LUMO-derived states, and the photoemission intensities seen here can be directly related to the real space distribution of the LUMO state of the isolated molecule.

B Beyond the Monolayer

To explore the development of the increase in photoemission intensity near E_F with molecular deposition beyond a monolayer coverage, series of ARUPS spectra were recorded for coverages of 3 Å (= 1 monolayer), 6 Å and 9 Å. These angular series are shown in Fig. S2 along with the corresponding LEED structure obtained at each coverage. The angular range of these series, $\theta = 14^\circ$ to 65° , corresponds to a k_y range of 0.5 to 1.9 \AA^{-1} , covering the region containing the Cu surface state and the new intensity at E_F associated with absorption. As observed in the main article, once the monolayer is completed, a highly ordered structure is formed, and the increase in intensity near E_F has developed fully into a strong feature arising from LUMO-metal hybridization.

C1s-NEXAFS measurements have been made to determine the phenyl plane tilt angle of the completed monolayer. The NEXAFS spectra in Fig. S3a show strong C1s $\rightarrow \pi^*$ resonance intensities at glancing incidence ($\theta = 80^\circ$) and no π^* intensity for normally incident X-rays ($\theta = 0^\circ$) in both azimuths. Such can only be the case if the phenyl ring, and hence the molecular plane are flat on the Cu(110) surface. In this situation, NEXAFS cannot reveal the azimuthal orientation of the long molecular axis. However, the LEED (Fig. S2a and Fig. 2a) results suggest and photoemission (Fig. 3b) and STM (Ref. [2] supplementary online material) results clearly show the long axis parallel to the $[1\bar{1}0]$ direction.

Beyond a coverage of one monolayer, as shown for two and three times the amount of material for a monolayer in Fig. S2b and c, respectively, the geometric structure of the film changes. Further, the strong photoemission features from the interface states around E_F first weaken at a coverage of 6 Å and then are gone by 9 Å as they are buried by a second layer of molecules.

In the NEXAFS spectra of a 9 Å coverage in Fig. S3b, the π^* resonance intensity in normal emission has appeared, revealing that this second layer has a significant tilt angle.

Analysis of the π^* resonance intensity with X-ray incidence angle yields an average tilt of $46^\circ \pm 2^\circ$ for the molecular phenyl plane. The near absence of π^* resonance intensity for polarization in the $[1\bar{1}0]$ azimuth at normal incidence reveals the orientation of the molecular axis along that azimuth, i.e. the azimuthal orientation of the molecules of thicker films is the same as the monolayer.

The LEED, ARUPS and NEXAFS measurements of coverages above a monolayer reveal that the LUMO-metal hybrid states exist only within the first monolayer of 6P on the metal surface. This flat wetting layer is then covered with a second wetting layer consisting of molecules of the same axial orientation but with a significant tilt of their phenyl planes with respect to the surface plane.

C Modifying the Periodicity

A different lateral periodicity to the full ML can be obtained by cooling sub-ML coverages to 100 K. The periodicity is reflected in a change in k -position of the paraboloids. It should be noted that the form of the parabolas is not changed, although the intermolecular distances are 10.8 Å and 7.2 Å for the sub-ML and full ML coverages, respectively. This result clearly indicates that the paraboloids are not a result of dispersion due to intermolecular overlap.

Series of ARUPS spectra were recorded for 0.5 ML 6P at 300 K (room temperature) and 100 K and 1 ML at 300 K in the Cu $\bar{\Gamma}$ - \bar{Y} direction. These angular series are shown in Fig. 4 along with the corresponding LEED structure obtained at each coverage.

As shown in the main article, the LEED of a 0.5 ML coverage on Cu(110) in Fig. 4a indicates that the incomplete ML is poorly ordered at room temperature, and the ARUPS series is somewhat featureless. The molecules maintain the alignment along the Cu[001] azimuth but are mobile. On cooling the 0.5 ML coverage to 100 K, both the LEED reflexes and the photoemission features become rather sharp (Fig. 4b). The sharpening of the features relative to those at room temperature indicates a reduction in the thermal motion (both translational and vibrational) of the incomplete molecular layer. The s,p band becomes visible again, and a remnant of the surface state appears in the bulk projected gap, suggesting that the 6P is forming 2D islands and leaving areas of Cu uncovered. Importantly, the periodicity of molecules in these islands is three Cu rows, which is different to the two Cu rows of the complete ML. As a result, the Cu-LUMO hybrid features at E_F display two parabolic features centered at $\theta = 44^\circ$ and 70° , or $k_y = 1.47$ and 1.99 \AA^{-1} , values 1/3 and 2/3 of the Cu Brillouin zone (BZ).

Once the ML is completed, a highly ordered structure is formed, as evidenced by the sharp reflexes of the LEED in Fig. 4c. The broad reflexes have changed from 1/3 to 1/2 of the underlying Cu periodicity, indicating that the side-to-side spacing of the molecules has changed from three Cu rows to two Cu rows with the increase in surface density.

D Theoretical Support

D.1 Orbital Character Calculation

Here we present density functional calculations for a 6P monolayer adsorbed on the Cu(110) surface using the SIESTA code [3]. We model the surface by 5 Cu-layers in a repeated slab approach where we fix the 6P monolayer distance to 2.4 Å and relax

the other structural degrees of freedom.¹ In addition, also calculations for the clean Cu(110) surface and an unsupported 6P monolayer have been performed. Fig. S5 shows the k -resolved projected density of states for these three systems: clean Cu(110) surface projected onto Cu d and Cu s (left), unsupported 6P projected onto C p_z (right), and 6P monolayer adsorbed to Cu(110) projected onto Cu d, Cu s, and C p_z (middle).

For the Cu slab calculations, the gap in the bulk projected density of states does not appear due to the folding of the Cu surface BZ in half. The electronic states of the unsupported 6P layer are flat and nearly nondispersive over the entire BZ, revealing little overlap between the orbitals of neighboring molecules in this geometry. Only when the 6P layer is combined with the Cu slab do the p_z features display appreciable dispersion. In particular, the former LUMO, HOMO and HOMO-1 all become less intense at any single energy value as they are spread over large ranges in energy through hybridization with substrate states. The LUMO molecular level is seen to cross E_F and display weak, but highly dispersive bands with roughly parabolic shapes below E_F in addition to an increase in dispersion in the unoccupied bands above E_F . The Cu d states are little perturbed by the addition of the 6P overlayer, but the s states show evidence of mixing with molecular levels. The s bands below the d band become less distinct, while some parabolic bands centered around the BZ boundary above the d band increase in intensity. The calculations clearly show a broadening of the π orbitals upon hybridization with the metal states. Experimentally, however, the degree of the loss of distinction in the energy of the π orbitals in the ML is difficult to ascertain due to their overlap with the Cu d band features.

D.2 Localized π orbitals

In Fig. S6, the calculated projected density of states (pDOS) [4] of the six localized orbitals (those with little overlap within the molecule, see main article and Ref. [1]) are displayed for the bound 6P monolayer on Cu(110) both in energy versus momentum and momentum-integrated representations. The calculations predict that these six molecular levels each split roughly into two bands separated by ~ 1 eV and lie at about the same binding energy. These orbitals, which lie at discrete energies in the unperturbed molecule, are clearly affected by the interaction with the Cu substrate. Their similar appearance as two somewhat discrete peaks all at about the same energy suggests that a degree of rehybridization is occurring when the symmetry is broken by the introduction of the Cu surface.

D.3 Torsional Angle

Fig. S7 displays a calculation of both a) the delocalized π band energy width (separation between HOMO to HOMO-11) and b) the total energy of an isolated 6P molecule as a function of torsional angle of the phenyl rings. In the calculation, the π band width increases about $\approx 22\%$ upon going from an isolated molecule with a torsional angle of $\approx 34^\circ$ to a planar conformation (0°). A comparison of the calculated torsional angle of isolated poly-*para*-phenylene (PPP) to crystalline PPP from Ref. [5] suggests that a reasonable torsional angle for crystalline 6P would be between 20° to 25° , leading to

¹Geometry optimization using standard GGA functionals gave a separation value of 2.8 Å but is known to overestimate the distance. No XSW measurements are available to accurately determine the distance. Several distances were tried and are similar in appearance and result in similar calculated interface dipole magnitudes.

only an $\approx 12\%$ increase in the π band spread for planar 6P over crystalline 6P. These calculations suggest that only 0.3 eV of the observed experimental difference in the π band spread of 2.7 eV and 3.9 eV for the crystalline and planar monolayer films, respectively, can be attributed to the difference in conformation. The remaining 0.9 eV then results from interactions of the π orbitals with the Cu substrate. Note that a comparison between the crystalline film here and the gas-phase spectrum of Ref. [6] with a band width of 2.5 eV is consistent with this analysis.

References

- [1] G. Koller, S. Berkebile, M. Oehzelt, P. Puschnig, C. Ambrosch-Draxl, F. P. Netzer, and M. G. Ramsey, *Science*, 2007, **317**(5836), 351–355.
- [2] P. Puschnig, S. Berkebile, A. J. Fleming, G. Koller, K. Emtsev, T. Seyller, J. D. Riley, C. Ambrosch-Draxl, F. P. Netzer, and M. G. Ramsey, *Science*, 2009, **326**(5953), 702–706.
- [3] J. Soler, E. Artacho, J. Gale, A. Garcia, J. Junquera, P. Ordejon, and D. Sanchez-Portal, *Journal of Physics-Condensed Matter*, 2002, **14**(11), 2745–2779.
- [4] G. M. Rangger, L. Romaner, G. Heimel, and E. Zojer, *Surface and Interface Analysis*, 2008, **40**(3-4), 371–378.
- [5] C. Ambrosch-Draxl, J. A. Majewski, P. Vogl, and G. Leising, *Physical Review B*, 1995, **51**(15), 9668–9676.
- [6] K. Seki, U. Karlsson, R. Engelhardt, E. Koch, and W. Schmidt, *Chemical Physics*, 1984, **91**(3), 459–470.

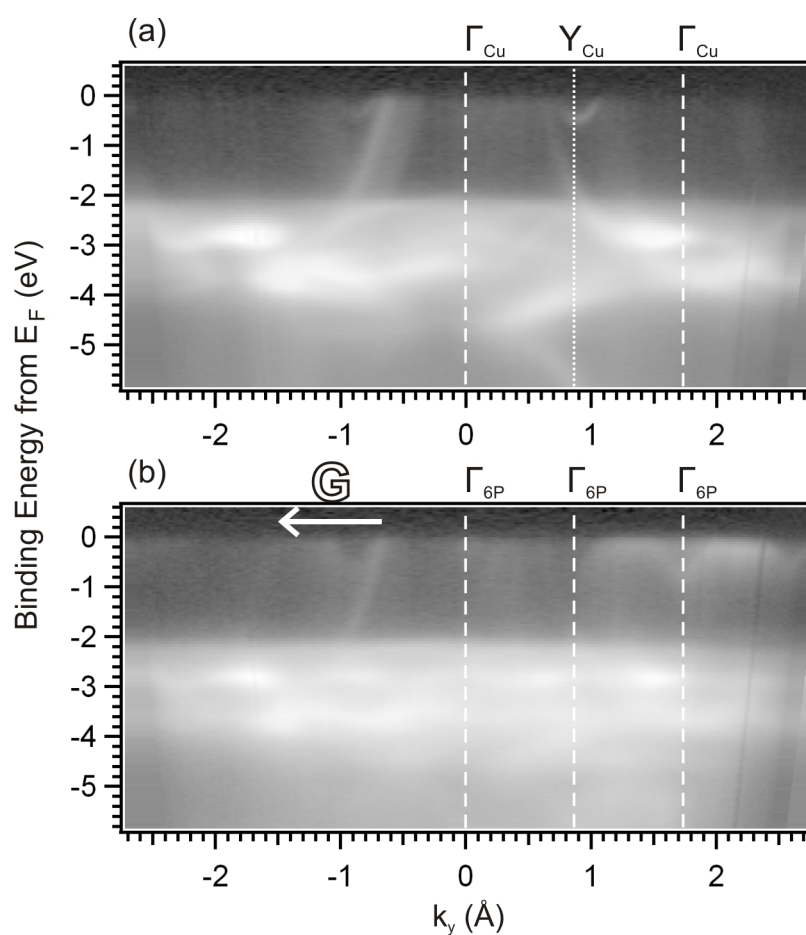


Figure 1: The $E(k_y)$ valence band maps (Cu[001], $\bar{\Gamma}$ to \bar{Y}) showing a) clean Cu(110) and b) Cu(110) with a monolayer of 6P. A logarithmic intensity scale has been used, black is the lowest intensity, white is the highest. The photon energy was $h\nu = 35$ eV and incidence angle $\alpha = 40^\circ$.

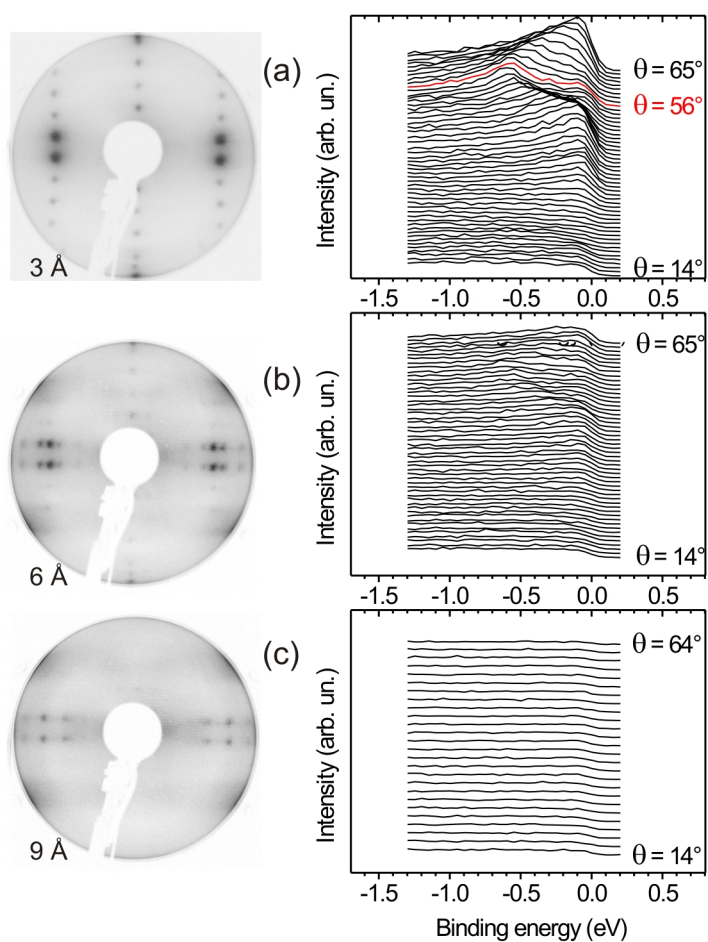


Figure 2: LEED images with a primary electron beam energy of 20 eV (left) and VB UPS spectra (right) near $E_F = 0$ eV for a) monolayer, b) 6 Å and c) 9 Å. UPS spectra were collected from 14° to 65° in 1° steps, except c) which has 2° steps. The intensity scales are the same for all and are thus directly comparable. Unpolarized HeI radiation was used (Photon energy $h\nu = 21.2$ eV) with an incident angle of $\alpha = 60^\circ$.

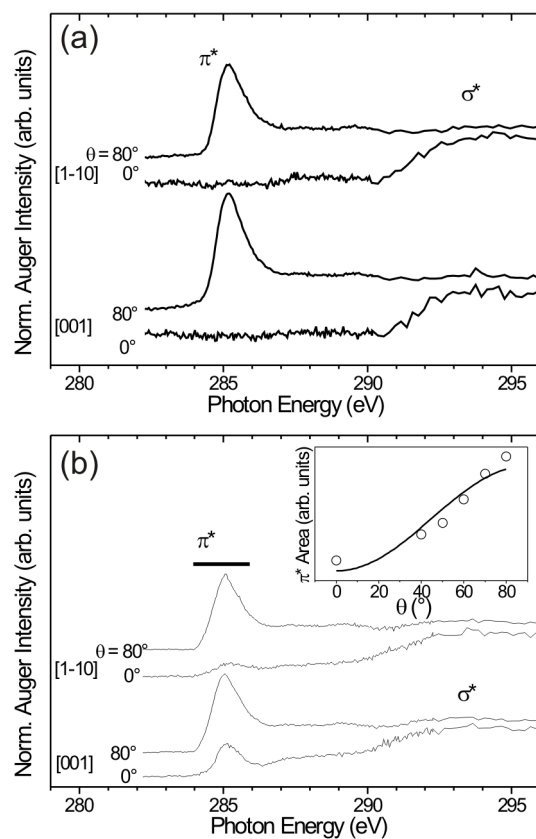


Figure 3: NEXAFS spectra of a) the full 6P monolayer and b) 9 Å 6P on the clean Cu(110) surface for X-ray polarization in the $[1\bar{1}0]$ and $[001]$ azimuthal directions for normal incidence ($\theta = 0^\circ$) and glancing incidence ($\theta = 80^\circ$).

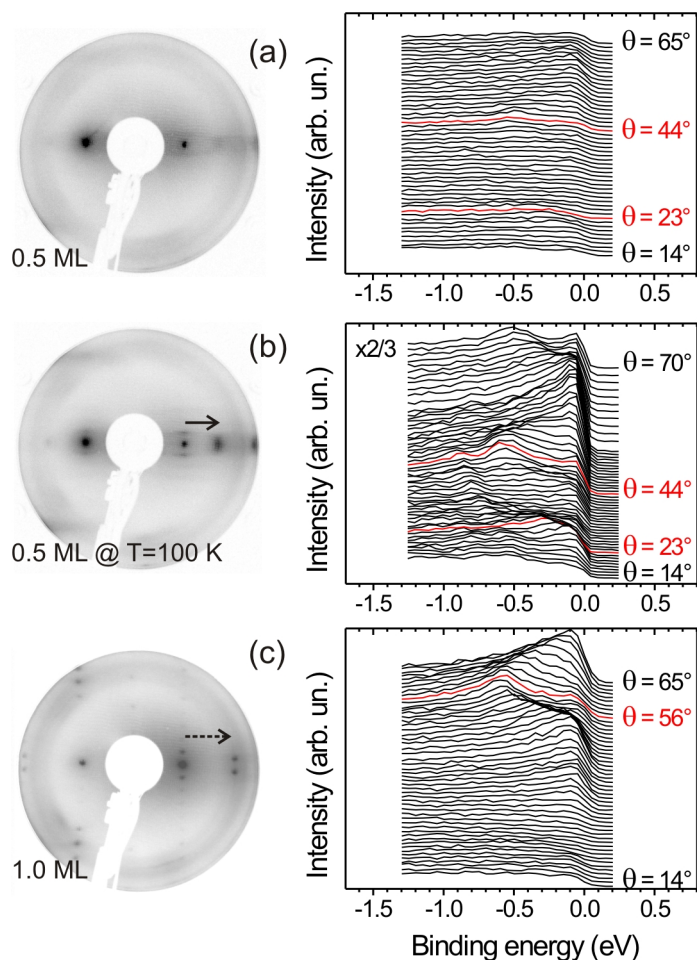


Figure 4: LEED images (left) and valence band UPS spectra near $E_F = 0$ eV (right) for a) 0.5 monolayer (ML) 6P at 300 K, b) 0.5 ML 6P cooled to 100 K and c) full ML 6P at 300 K. UPS spectra were collected for emission angles from 14° to 65° in 1° steps (roughly 0.5 to 1.9 \AA^{-1}), except b) which extends to 70° . The intensity scales are the same for all except b) which was multiplied by $2/3$. Unpolarized HeI radiation was used (Photon energy $h\nu = 21.2$ eV) with an incident angle of $\alpha = 60^\circ$. A primary beam energy of 50 eV was used for LEED. Solid arrows have a length $1/3$ of the Cu reciprocal lattice vector, and dashed arrows $1/2$.

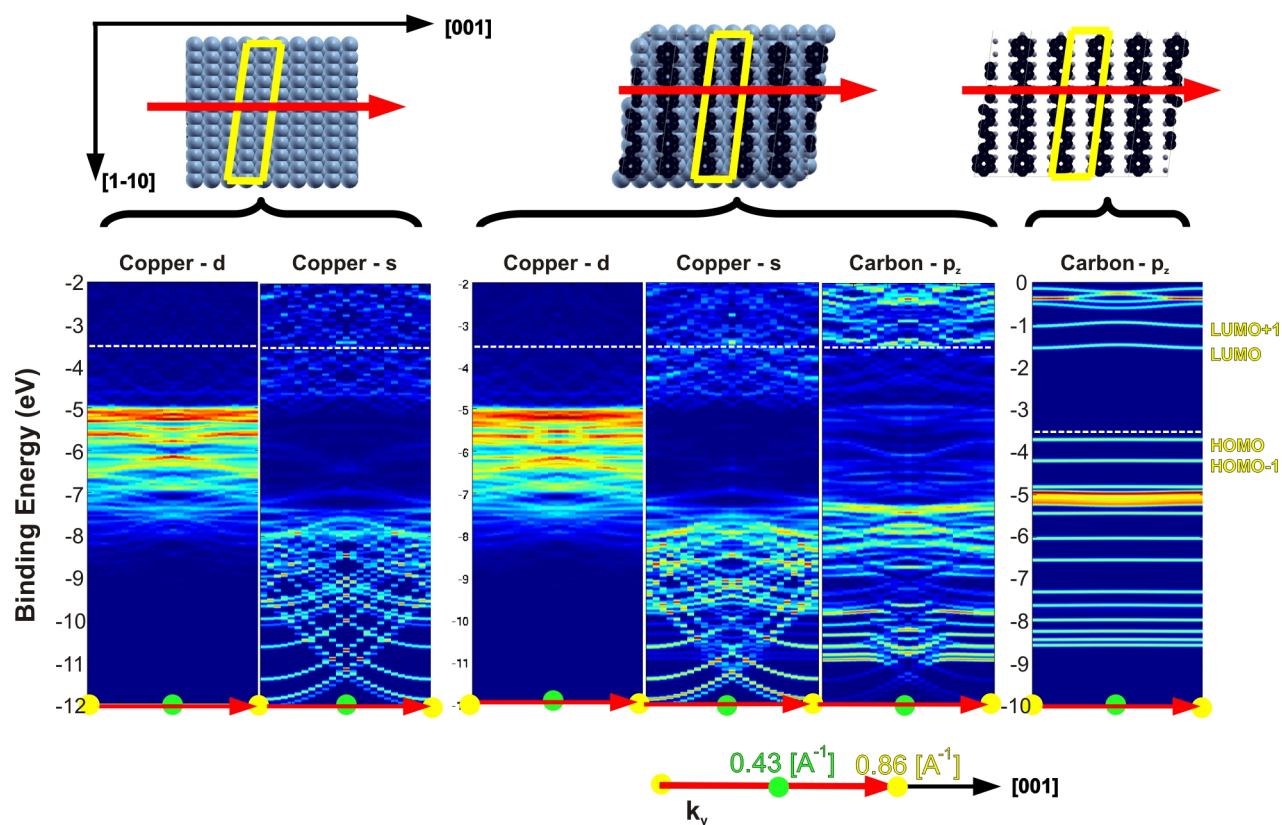


Figure 5: Calculation of the $E(k)$ behavior in the Cu $\bar{\Gamma}$ to \bar{Y} direction of electron levels with Cu d, Cu s and C p_z character for a Cu slab (left), combined Cu-6P system (center) and unsupported 6P layer (right) assuming a BZ determined by the overlayer periodicity. The Fermi level is shown by a white dashed line.

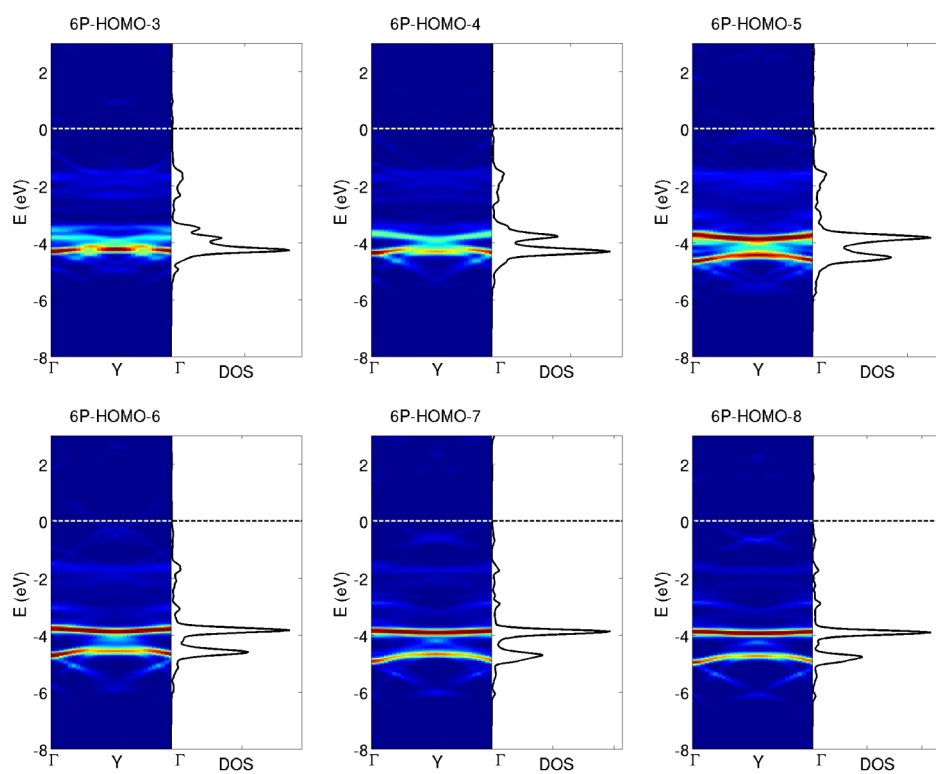


Figure 6: Calculation of the electronic structure projected onto the localized π orbitals in $E(k)$ (left) and k -integrated (right).

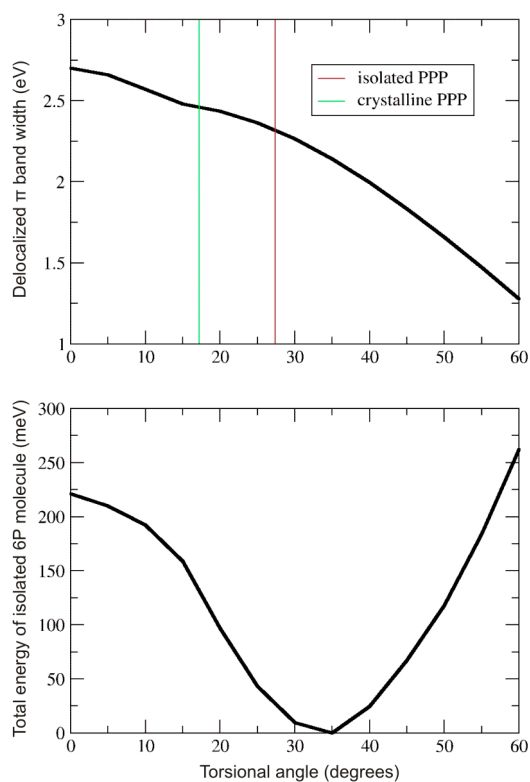


Figure 7: Calculation of the delocalized π band. (a) π band energy width (HOMO to HOMO-11 energy spread) and (b) total energy of an isolated 6P molecule as a function of phenyl ring torsional angle. The minimum total energy of isolated and crystalline poly-*para*-phenylene (PPP) from Ref. [5] has been added to (a) for reference.